

NUMERICAL MODELLING OF WOOD FRAME JOINTS HAVING FIRE STOPS

T.R.T. Nightingale

Acoustics Laboratory, Institute for Research in Construction,
National Research Council Canada, Ottawa Ontario K1A 0R6

Robert J.M. Craik

Department of Building Engineering and Surveying,
Heriot Watt University, Riccarton, Edinburgh UK EH14 4AS

Introduction

In a companion paper¹ the degradation of the net air borne sound isolation resulting from the flanking path caused by a special class of fire stops was investigated. This paper will examine a simple model for the propagation of bending waves through the joint involving a fire stop constructed by continuing one of the room's surfaces across or under the nominally separating element. Figure 1 shows a simplified section through the partition wall and the end wall that will be modelled. Due to the symmetry of the joint it can be viewed as a pair of corner joints coupled by an element (i.e., the fire stop) having a unique bending stiffness. In the simplified model presented here, only the transverse component of the surface velocity will be considered as it is this motion (i.e., that caused by bending waves) that will be, by far, the most effective at converting structural vibration to airborne acoustic energy.

Joint Equations

In deriving the equations for the joint it is assumed that each corner is pinned (i.e., there is no translational motion) and the fire stop that couples the corner joints has only stiffness. This is not the case in reality as the fire stop usually has a width equal to the 25 mm nominal gap left in double stud walls. The effects of the studs at the joint will not be considered as their treatment will introduce wave types other than bending waves. A mechanical representation of the simple system is shown in Figure 2. If the corner joints are assumed to be pinned rigid then the following equations of motion can be written,

$$\phi_1 = -\phi_2 \text{ and } \phi_3 = -\phi_4, \quad [1a]$$

$$M_1 - M_2 + \hat{M} = 0 \text{ and } M_3 - M_4 - \hat{M} = 0, \quad [1b]$$

where ϕ is the angular rotation, and M is the moment. The subscript indicates the arm of the joint (as per Figure 1) while the circumflex refers to the fire stop material that connects the two corner joints. If the bending wave enters the joint from arm 1 then the following equations define the transverse displacement, ξ , in each arm,

$$\xi_1 = \left(e^{-ik_1 x \cos \theta_1} + T_1 e^{+ik_1 x \cos \theta_1} + T_{n1} e^{+k_{n1} x} \right) e^{-ik_1 y \sin \theta_1}, \quad [2a]$$

$$\xi_2 = T_2 e^{-ik_2 z \cos \theta_2} + T_{n2} e^{-k_{n2} z}, \quad [2b]$$

$$\xi_3 = T_3 e^{-ik_3 x \cos \theta_3} + T_{n3} e^{-k_{n3} x}, \quad [2c]$$

$$\xi_4 = T_4 e^{ik_4 z \cos \theta_4} + T_{n4} e^{k_{n4} z}, \quad [2d]$$

where T is the amplitude of the bending wave on the arm indicated by the subscript, the 'n' of the subscript indicates the near field or evanescent wave, k is the wavenumber for travelling waves, k_n is the wavenumber for the evanescent waves and θ is the angle of propagation. The displacements given in Equation[2] are related to Equation[1] by,

$$\phi_1 = \frac{d\xi_1}{dx} \text{ and } M_1 = -B_1 \left[\frac{d^2 \xi_1}{dx^2} + \mu \frac{d^2 \xi_1}{dy^2} \right], \quad [3]$$

where B is the bending stiffness of the arm and μ is Poisson's ratio. Equations[1], [2] and [3] represent a set of four simultaneous equations involving the eight unknown coefficients. The additional four equations required for a unique solution can be realized by considering the constraint placed on the motion at the joint. This motion must be purely rotational (i.e., the displacement is zero at $x=z=0$). This gives,

$$T_1 + T_{n1} = -1, \quad T_2 + T_{n2} = 0, \quad T_3 + T_{n3} = 0, \quad [4]$$

and $T_4 + T_{n4} = 0.$

Now a set of eight simultaneous equations can be created to describe the amplitude of the bending waves in each of the four arms. The resulting matrix for the case of normal incidence is Equation[5] (shown on next page).

Fire Stop Modelling

Equation[5] was used to calculate the velocity level difference or velocity transmission loss across the joint shown in Figure 1. The effective bending stiffness of the fire stop material is given by,

$$\hat{B} = \frac{Et^3}{(1 - \mu^2) d} \quad [6]$$

where E is Young's Modulus, μ is Poisson's ratio, and d is the span of the fire stop. (Typically this is about 25 mm since this is the distance between plates in a double stud wall.) The predicted surface velocity transmission loss at normal incidence between arms 1 and 3 (TL_{13}) is shown in Figure [3] for a few possible fire stops. Due to symmetry in constructions of arms 3 and 4, $TL_{13} = TL_{14}$. (Each arm had

a bending stiffness per unit width of 340 Nm.) From the figure it is evident that the TL across the joint is a function of both stiffness and frequency. The 0.38 mm sheet steel fire stop, having very little bending stiffness, offers the best vibration isolation with the TL increasing 6 dB per doubling of frequency. Comparing the TL for 13 mm gypsum board with spans of 8 mm and 25 mm one can see that reducing the span of the fire stop reduces the TL. A fire stop made from two layers of 13 mm gypsum board only provides slightly better TL than a single layer of 16 mm plywood. For the

frequency range 100 to 100 Hz the plywood fire stop is only marginally better than if the joint were perfectly rigid (i.e., a cross joint). It should be noted that the surface velocity transmission losses given here can not be compared directly to standard measures of airborne sound reduction (i.e., ASTM E90 or E336 which are measures of sound power reduction). This is due to the fact that sound power accepted/radiated by a surface is related to the surface velocity through the radiation factor which has not been considered in this discussion.

$$\begin{bmatrix} ik_1 & k_{n1} & ik_2 & k_{n2} & 0 & 0 & 0 & 0 & 0 & 0 \\ 0 & 0 & 0 & 0 & -ik_3 & -k_{n3} & -ik_4 & -k_{n4} & 0 & 0 \\ B_1 k_1^2 - i\hat{B}k_1 & -B_1 k_{n1}^2 - \hat{B}k_{n1} & -B_2 k_2^2 & B_2 k_{n2}^2 & -i\hat{B}k_3 & -\hat{B}k_{n3} & 0 & 0 & 0 & 0 \\ i\hat{B}k_1 & \hat{B}k_{n1} & 0 & 0 & -B_3 k_3^2 + i\hat{B}k_3 & B_3 k_{n3}^2 + \hat{B}k_{n3} & B_4 k_4^2 & -B_4 k_{n4}^2 & 0 & 0 \\ 1 & 1 & 0 & 0 & 0 & 0 & 0 & 0 & 0 & 0 \\ 0 & 0 & 1 & 1 & 0 & 0 & 0 & 0 & 0 & 0 \\ 0 & 0 & 0 & 0 & 1 & 0 & 0 & 0 & 0 & 0 \\ 0 & 0 & 0 & 0 & 0 & 1 & 0 & 0 & 0 & 0 \\ 0 & 0 & 0 & 0 & 0 & 0 & 1 & 1 & 0 & 0 \end{bmatrix} X = \begin{bmatrix} T_1 \\ T_{n1} \\ T_2 \\ T_{n2} \\ T_3 \\ T_{n3} \\ T_4 \\ T_{n4} \end{bmatrix} = \begin{bmatrix} ik_1 \\ 0 \\ -B_1 k_1 - i\hat{B}k_1 \\ i\hat{B}k \\ -1 \\ 0 \\ 0 \\ 0 \\ 0 \end{bmatrix} \quad [5]$$

Conclusions

To optimize the sound isolation of partition assemblies having fire stops, it is critical to select the correct fire stop material. This is especially true when high degrees of sound isolation are required. The structural decoupling (hence superior sound isolation) gained by using a double stud wall may be completely defeated if a very stiff fire stop is used. The only way to maximize the airborne transmission loss of a partition is to use a fire stop whose effective bending stiffness is very much lower than the bending stiffness of the surfaces to which it is connected. Thus, of all the materials listed in the NBCC, the 0.38 mm sheet steel is most likely to satisfy this criterion and offer the greatest sound isolation. The span of the fire stop should be maximized where possible.

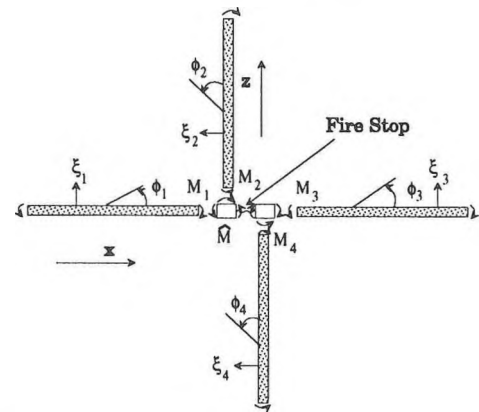


Figure 2: Mechanical representation of the joint.

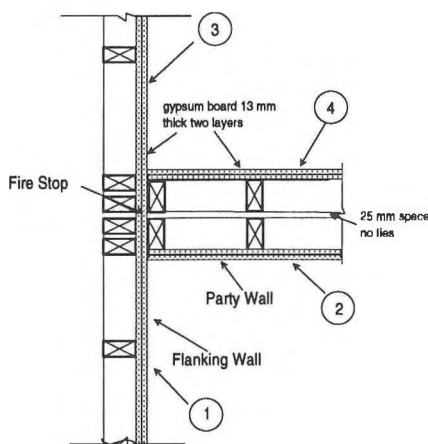


Figure 1: Plan section through the joint.

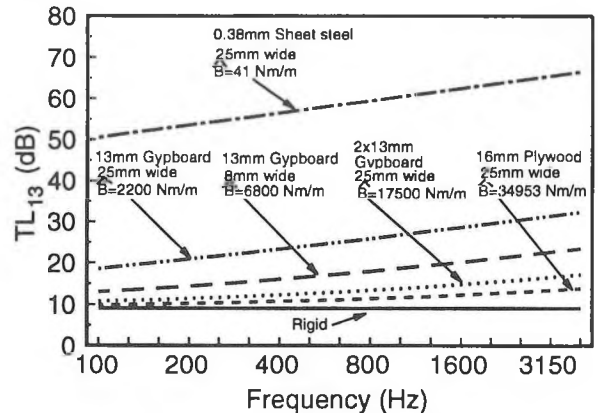


Figure 3: Predicted normal incidence velocity transmission loss for the paths 13 and 14 obtained from Equation 5. Effective bending stiffnesses of the fire stops are given in N-m/m.

¹Flanking Transmission Caused by Fire Stops in Wood Frame Constructions, Proceedings Issue of the 1994 Canadian Acoustical Association Conference, Ottawa, 1994.